ELSEVIER

Coastal Engineering 38 (1999) 261–273

COASTAL ENGINEERING

www.elsevier.com/locate/coastaleng

Technical note

Flow resistance in the coastal zone

K.T. Houwman [a,*], L.C. Van Rijn [a,b]

[a] *Institute for Marine and Atmospheric Research Utrecht, Department of Physical Geography, Utrecht University, P.O. Box 80.115, 3508 TC Utrecht, Netherlands*

[b] *Delft Hydraulics, Delft, Netherlands*

Received 16 February 1998; accepted 23 June 1999

Abstract

The apparent bed roughness, the roughness value experienced by a mean flow outside the wave-boundary layer, is deduced from the physical bed roughness and the wave–current interaction mechanism. Both the physical bed roughness and the wave–current interaction are described by a (combination of) model(s). Modelling of the apparent bed roughness leads to realistic results, however, the final results are rather sensitive to the particular choice of these models. Four bed form models and two wave–current interaction models were implemented in a 1-DV flow model to calculate near-bed velocities. A comparison between measured and predicted velocities shows that reasonable results can be obtained in this way. A constant bed roughness of 0.1 m, however, leads to even better results at this site during all conditions. This can be explained by the reversed influence of the form roughness and the wave–current interaction on the apparent bed roughness value for varying wave conditions.

Keywords: Bed roughness; Bed forms; Wave–current interaction; Flow model; Tidal flow

1. Introduction

In the last decades, many numerical flow models have been developed describing the flow field in coastal seas. In general, these models need a roughness length (z_0) or bed roughness (Nikuradse roughness $k = 30\ z_0$) to determine the bottom boundary conditions for the flow equations. This roughness parameter, which is actually a schematisation of several physical processes in a thin layer close to the bed, is difficult to determine in field conditions, because it is influenced by many variables. First of all, the fluid motion over a bed consisting of sand is influenced by the presence of the grains on

* Corresponding author. Tel.: +31-30-2532753; fax: +31-30-2531145; E-mail: k.houwman@geog.uu.nl

0378-3839/99/$ - see front matter
PII: S0378-3839(99)00049-6

the bottom. This creates a shear effect, parameterised by the bed roughness. Furthermore, the fluid–sediment interaction over a movable bed results in the generation of bed forms, which act as roughness elements to the flow. The dimensions of these bed forms, which are important for the actual roughness value, are influenced by both currents and waves. So, in field conditions, this shear effect will change in time. An increase of the energy conditions above a certain level result in the flattening of the bed forms, the sheet flow regime. Large sediment concentrations are generated under these conditions creating an additional friction effect for the flow. This mechanism can also be expressed as an increased roughness value (Grant and Madsen, 1982). The situation becomes even more complex if both waves and currents are present. In that case, the shear stress and turbulence intensities in the wave boundary layer are due to the combined effect of both wave and current, which are coupled in a non-linear fashion. The result is that the current in the region above the wave boundary layer experiences a shear stress, which depends on wave boundary layer characteristics and will be different from the shear stress in a pure current situation. This process can be schematized by an apparent roughness value experienced by the flow above the wave boundary layer.

Although in literature a lot of empirical and theoretical work is described about this subject, no generally accepted method is available to describe the apparent roughness value in field conditions in the presence of waves and currents.

The objective of this paper is to show a way in which the apparent bed roughness can be calculated using existing bed roughness sub models and which can hopefully serve as a helping hand to coastal modellers. Furthermore, the influence of the different components contributing to the apparent bed roughness is investigated. Finally, predicted flow velocities obtained from a flow model using different combinations of bed roughness sub models are compared with measured flow velocities. The evaluation of these results give insight in the accuracy of flow predictions using different bed roughness formulations.

2. Description of the field site and measurements

The flow measurements, which are used for the evaluation of the flow model were made in the multiple bar system at the barrier island Terschelling, the Netherlands, within the frame work of the NOURTEC project (Hoekstra et al., 1994). The field site is fully exposed to the North Sea, with an average annual offshore wave height of 1.1 m. Tides are semi-diurnal with a neap tidal range of about 1.2 m and a spring tidal range of about 2.8 m. Tidal ellipses are orientated shore parallel and are almost flat at least within a distance of 2 km from the shoreline. The inner near shore zone is characterized by several breaker bars parallel to the shoreline. These bars are more or less uniform in longshore direction in the area of interest. The grain size varies in cross-shore direction, and the median grain size (D_{50}) at positions P1 and P2 is 155 and 165 μm, respectively. The corresponding D_{90}-values are 205 and 220 μm. Instrumented tripods were placed in a cross-shore profile at two position P1 and P2 at depths of 9 and 5.5 m. Data was collected over a time period of 2 years. Both tripods were equipped with two Electro Magnetic Flow meters (EMF) at (nominal) heights of 0.3 and 1.2 m above the bed and a

pressure sensor at 2.2 m above the bed. A total amount of 2682, 9220 bursts of validated data was gathered at the positions P1 and P2, respectively. The data is used in Section 7 in which a comparison between predicted and measured velocities is carried out.

3. The flow model

In this study, a one-dimensional vertical flow model (1-DV) will be used for evaluation of selected bed roughness methods. Details and an evaluation of this model are presented by Houwman and Uittenbogaard (1999). This 1-DV flow model describes the horizontal velocity vector over the water column at a single location in the horizontal plane. The equations of motion in cross-shore and longshore direction at a particular height z above the bottom are respectively given by Eqs. (1) and (2).

$$\frac{\partial u}{\partial t} = -g\frac{\partial \zeta}{\partial x} + fv + \frac{\partial}{\partial z}\left(\nu_T \frac{\partial u}{\partial z}\right) \tag{1}$$

$$\frac{\partial v}{\partial t} = -g\frac{\partial \zeta}{\partial y} - fu + \frac{\partial}{\partial z}\left(\nu_T \frac{\partial v}{\partial z}\right) \tag{2}$$

In these flow equations, u and v are the orthogonal velocity components in x (cross-shore) and y (longshore) direction, respectively, and ζ is the surface elevation above mean sea level. The Coriolis parameter $f = 2\Omega\sin\Phi$ represents the influence of the earth's rotation. The eddy viscosity ν_T is calculated from the Kolmogorov–Prandtl expression, using a standard k–ϵ turbulence model. The bottom boundary condition for Eq. (1) reads:

$$\nu_T \frac{\partial u}{\partial z}\bigg|_{z=z_0} = S^2 u\sqrt{u^2 + v^2}\,. \tag{3}$$

The friction factor S is given by $S = \kappa/\ln(z_1/z_0)$, with κ the Karman constant. Similar conditions are used at the upper boundary as well as for Eq. (2). To drive the model, the observed longshore surface gradient is used. This gradient is deduced from measured water levels at two locations (at distance of 41.3 km) along the coast.

The depth-integrated version of Eq. (1) is used to calculate the cross-shore surface gradient $\partial\zeta/\partial x$. A stable consistent solution will be obtained when Eqs. (1) and (2) and the depth-integrated version of Eq. (1) are solved subsequently. To apply this method, the depth-averaged cross-shore current has to be specified and is here taken equal to zero. Finally, specification of the roughness length z_0 is needed to apply the model. The roughness length is related to the apparent bed roughness k_a by $z_0 = k_a/30$.

4. The physical roughness

4.1. Introduction

In a pure current situation without waves, the bed roughness is known as the physical roughness. This physical roughness k_p is the end result of the skin friction forces acting

on the non-moving bed material (grain roughness), the pressure forces acting on bed forms (form roughness) and drag forces on the moving sediment grains in the near-bed transport layer (transport related roughness). All three terms can be expressed in terms of an effective sand roughness height according to the Nikuradse concept and are referred to as k_g, k_f and k_t, respectively. In line with the work of Grant and Madsen (1982), Nielsen (1992) and Van Rijn (1993), the total physical bed roughness k_p is taken as the sum of these three components: $k_p = k_g + k_f + k_t$. The roughness due to the presence of the bed material (k_g) is about equal to 3 D_{90} according to Van Rijn (1993).

4.2. Form roughness

Form roughness is the roughness produced by the bed forms. In the near shore zone, during calm to moderate energetic conditions both small-scale ripples and mega-ripples have been found. During more energetic conditions, the bed forms are washed out and large sediment concentrations above the bed occur (sheet flow). Generally, bed forms are influenced by both waves and currents. Herein it is assumed that bed forms in the near shore zone are dominated by wave motions. Furthermore, only small scale ripples are taken into account.

The form roughness k_f can be calculated from the ripple height η, the ripple length λ using the relationships of Nielsen (1981), Grant and Madsen (1982) and Van Rijn (1993): $k_f = \alpha\eta(\eta/\lambda)$ with α in the range from 8 (Nielsen, 1981) to 27.7 (Grant and Madsen, 1982). Four methods have been applied here for calculating the bed form dimensions. The methods applied in this study are: Nielsen (1981), Grant and Madsen (1982), Van Rijn (1993) and Li et al. (1996).

To get some insight in the differences between these models, computations have been carried out for a range of peak orbital velocities in combination with three different wave periods ($T = 6$, 12 and 18 s). For these computations, the mean flow velocity was taken equal to zero and a median grain size D_{50} of 160 μm was used. Fig. 1 shows the ripple height and length and the form roughness for each bed form model.

For all models, the ripple height is increasing rapidly with the peak orbital velocity and for $T = 6$ s its maximum is found at about 0.15 m/s for the Nielsen (1981) model and around 0.25 m/s for the other models. As can be seen in Fig. 2, the ripple height is rather sensitive to the wave period. The bed form models of Nielsen (1981) and Van Rijn (1993) predict a transition from the ripple regime to the sheet flow regime at an orbital velocity between 0.5 and 0.75 m/s. In the sheet flow regime, the ripple height predicted by these models is zero. The ripple height predicted by the Grant and Madsen (1982) and the Li et al. (1996) model is slowly decreasing for an increasing peak orbital velocity. Large differences are found in the predicted values for the ripple length for the different models. The predicted ripple length is also rather sensitive for the wave period.

Finally, the form roughness, calculated from the ripple dimensions, is shown in Fig. 1. The form roughness is calculated using $k_f = \alpha\eta(\eta/\lambda)$ with $\alpha = 8$ (Nielsen, 1992), $\alpha = 20$ (Van Rijn, 1993), and $\alpha = 27.7$ (Grant and Madsen, 1982; Li et al., 1996). The maximum values of the form roughness, shown in Fig. 1, coincide more or less with the peak in the ripple height distribution. The roughness values, predicted by the Van Rijn (1993) and Li et al. (1996) model are comparable for peak orbital velocities < 0.5 m/s. The Grant and Madsen (1982) model produces much larger roughness values than the

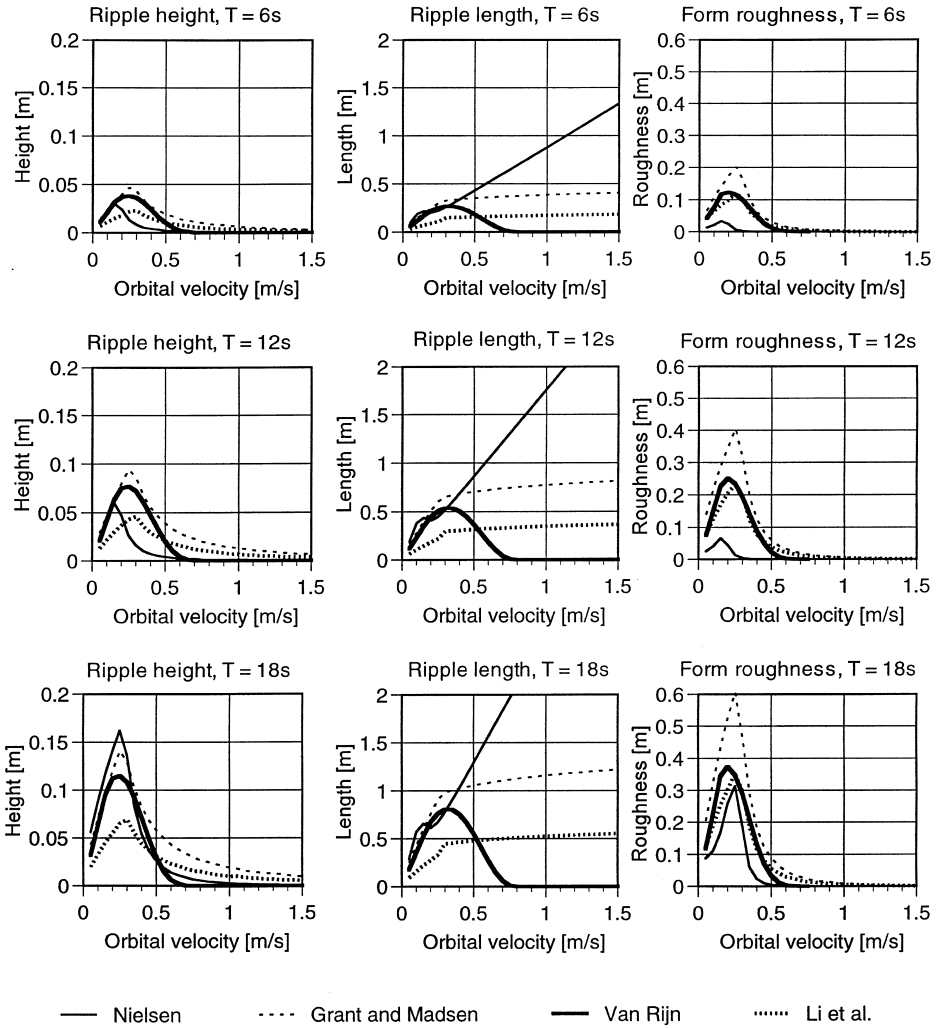

Fig. 1. The predicted bed form dimensions and form roughness, resulting from four bed form models.

other models. The Nielsen (1981) model produces the smallest roughness values. There is, however, one exception, the form roughness predicted by the Nielsen model is comparable to the Van Rijn (1993) and Li et al. (1996) model for the case $T = 18$ s. The Nielsen (1981) model predicts a rapid increasing roughness value for high wave periods. The other three models show an almost linear relationship between the peak orbital velocity and the form roughness. The differences between the predicted roughness values are both due to the differences in the predicted bed form dimensions as well as in the different values for α applied in the computations of the form roughness.

In the sheet flow regime, orbital velocity > 0.5–0.6 m/s, the form roughness predicted by the Nielsen (1992) and the Van Rijn (1993) models becomes nil, while the

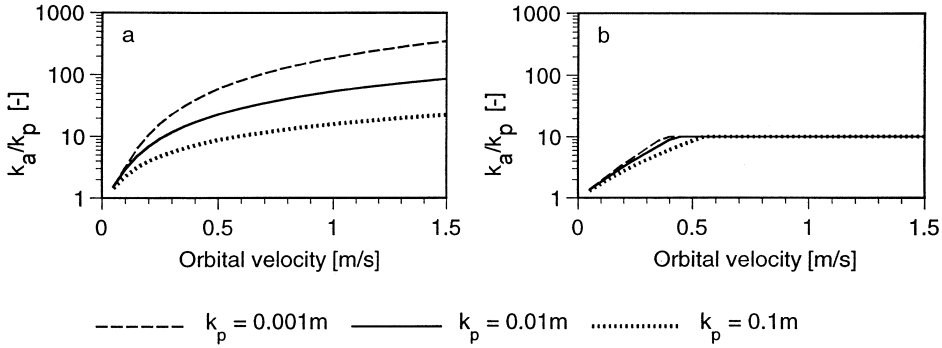

Fig. 2. The ratio between apparent roughness and physical roughness for the Grant and Madsen (a) and the Van Rijn (b) WC-model.

other two theories come up with roughness values in the order of O (1 mm). Although the Van Rijn model predicts no form roughness value in the sheet flow regime, Van Rijn (1993) recommends a minimum physical roughness value equal to $k_p = 0.01$ m for field conditions to represent small irregularities along a ''plane'' sheet flow bed.

4.3. Bottom roughness due to near-bed sediment transport

The physical roughness over a flat bed during sheet flow conditions will be enhanced due to the interaction between the moving sediment particles and the flow. The turbulent forces are continuously accelerating the sediment grains which are rising and falling in the near-bed layer. As a result, fluid momentum is transferred to the particles modifying the shear velocity. This mechanism can be described by an additional roughness, the transport-related roughness k_t. Three formulations describing this mechanism are evaluated in this study, namely the approaches suggested by Grant and Madsen (1982), Nielsen (1992), and Van Rijn (1993). Analysis of unidirectional flow data over a plane bed in the high-concentration range with sheet flow (velocities up to 3 m/s) shows that the overall bed roughness (including transport-related roughness) is of the order of 10 to 30 D_{90} (Van Rijn, 1993). In oscillatory flow over a plane bed with sheet flow, the transport-related roughness should be of the order of the thickness of the sheet flow layer, which roughly is of the order of 0.01 m or about 30 D_{90} for sediment of 0.2 to 0.3 mm (Ribberink and Al-Salem, 1994). The relationships presented by Grant and Madsen (1982) and Nielsen (1992) produce values which are an order of magnitude larger. Both methods have been derived from the same wave tunnel data set in the ripple regime (Carstens et al., 1969) using transport related roughness as a closing term. Plane bed tests in the sheet flow regime were not done by Carstens et al. (1969). Therefore, the relationships of Grant and Madsen (1982) and Nielsen (1992) should be used with caution. A similar conclusion was given by Li and Amos (1998). Computations have been made for some typical conditions using these formulations to demonstrate the differences between these methods. For these computations, the grain size parameter D_{90} is taken equal to 210 μm. The values predicted by the Grant and Madsen (1982) method are found to be approximately 100 times larger than the roughness values

predicted by the Van Rijn (1993) method under sheet flow conditions, which is a rather striking result. Given the uncertainties involved, the transport-related bed roughness is not further considered in this paper.

5. Wave–current interaction and apparent roughness

Several authors describe the interaction between waves and currents in the wave boundary layer (e.g., Grant and Madsen, 1979, 1986; Soulsby et al., 1993; Van Rijn, 1993). In the wave boundary layer, the shear stress is the result of the turbulence generated by both waves and the mean flow. The influence of waves on the turbulence intensity (shear stress), however, is rather large compared to that of a current as a result of the strong vertical gradient of the orbital velocity in this layer. According to the concept given by Grant and Madsen (1979), the flow profile is determined by the combined (waves and current) shear stress. The mean flow inside the wave boundary layer is affected by the additional mixing in this layer, giving a smaller current value at the upper edge of the wave boundary layer. The current above this boundary layer is affected by the shear stress of the current alone. The velocity profile above the wave boundary layer, however, exhibits smaller values in the case with waves than without waves. This effect can be expressed by a larger roughness (apparent roughness) value which is experienced by the current above the wave boundary layer in the presence of waves.

In this study, two wave–current interaction models (WC-models) describing this effect are applied, the detailed mathematical–physical Grant and Madsen (1979) model and the semi-empirical engineering method proposed by Van Rijn (1993).

The Van Rijn (1993) model is based on an analysis of experimental data from flumes with rippled beds. In the proposed formulation, the apparent bed roughness depends on the ratio of the peak orbital velocity and the mean flow velocity. In this model, the (k_a/k_p)-ratio is limited to a value equal to 10 (experimental range considered).

Computations were carried out applying both models for typical conditions. The ratio between apparent roughness and physical roughness as a function of the peak orbital velocity is shown in Fig. 2. These computations are based on a mean flow velocity of 0.2 m/s at 0.3 m above the bed, a water depth of 8 m, wave direction perpendicular to the flow direction and for three physical roughness values.

The results presented in Fig. 2, indicate that the amplification factor k_a/k_p, predicted by the Grant and Madsen (1979) method is larger than that by the Van Rijn (1993) formulation, for peak orbital velocities < 0.5 m/s. The latter method applies a maximum apparent roughness equal to 10 times the physical roughness.

6. Computation of the apparent bed roughness

To obtain some insight into the behaviour of the computed apparent roughness as a function of the near-bed velocities, computations have been made for a standard case representing a typical condition at the Terschelling site (see Section 2). The computa-

tions presented here were made using a $D_{50} = 160$ μm, $D_{90} = 210$ μm, water depth = 8 m, wave period = 6 s and using a wave propagation direction perpendicular to the current direction. The physical bed roughness was computed from the grain roughness and one of the bed form models. The transport-related bed roughness is not considered. The apparent bed roughness is obtained from one of the two WC-models using the computed physical roughness. Fig. 3 shows the apparent bed roughness as a function of the near-bed wave orbital velocity computed using the Grant and Madsen (1979) WC-model and the van Rijn WC-model. These results were obtained using a mean flow velocity of 0.2 m/s at 0.3 m above the bed. The results presented here indicate that the use of the Grant and Madsen, the Van Rijn and the Li et al. bed form model leads to comparable apparent roughness values up to an orbital velocity of approximately 0.8 m/s. Above this limit, the minimum physical roughness value proposed by Van Rijn, $k_{p,minimum} = 0.01$ m, leads to significant larger roughness values than the other two methods. In the ripple regime (peak orbital velocity < 0.5 m/s), the computed roughness values according to the Van Rijn WC-model are slightly smaller than for the Grant and Madsen (1979) WC-model. For orbital velocities above about 0.5 m/s, the apparent roughness values obtained from the computations using the Grant and Madsen and Li et al. bed form models decrease with increasing wave orbital velocity, while the two other methods leads to a constant value. This different behaviour is due to the clipping of the k_a/k_p ratio in this WC-model.

An important effect which is noticeable in Fig. 3 is the stabilisation of the apparent bed roughness over a wide range of orbital velocities due to the behaviour of the physical roughness. The principle of this is shown in Fig. 4. Here, the physical roughness k_p, the k_a/k_p ratio and the apparent bed roughness k_a are shown computed from the Grant and Madsen bed form and the Grant and Madsen WC-model. In the ripple regime, the rather high physical roughness is combined with a rather small k_a/k_p ratio representing the wave–current interaction effect, while in the sheet flow regime, a small physical roughness is combined with a large amplification effect due to the wave–current interaction. This mechanism reduces the range of the apparent bed

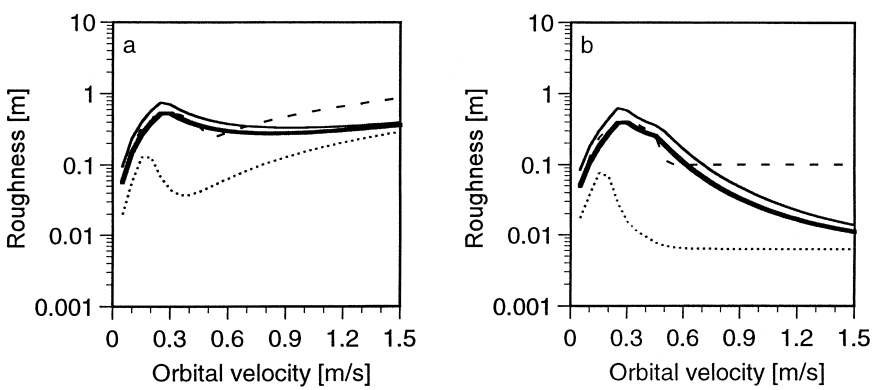

Fig. 3. Apparent roughness values calculated with the Grant and Madsen WC-model and van Rijn WC-model and four bed form models.

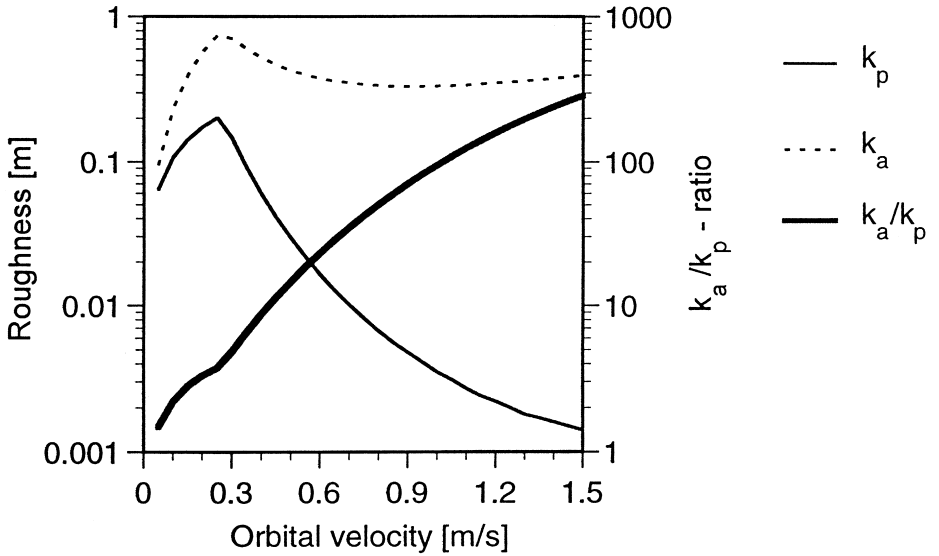

Fig. 4. Example of predicted apparent roughness value.

roughness compared to a case with a fixed physical bed roughness. Another effect, which plays a role in the stabilization of the apparent roughness, is the sensitivity of the WC-model(s) to the physical bed roughness (see Fig. 2). Both WC-models predict a decrease of the k_a/k_p ratio for an increase of the physical roughness. Therefore, relative differences between the apparent roughness values computed from different bed form models are smaller than the relative differences between the corresponding physical roughness values.

7. Application of the 1-DV flow model using different roughness scenarios

The roughness submodels presented in Sections 3 and 4 have been implemented into the 1-DV flow model. The flow model is run for two selected periods for the locations P1 and P2 along the barrier island of Terschelling, the Netherlands (see Section 2). A comparison between measured and predicted velocities at 0.3 m and at 1.2 m above the bed will give insight in the usefulness of a particular combination of roughness models for flow-models in field situations. From the data set, two time periods, with a total length of 215 h of velocity data were selected dealing with calm to moderate weather conditions (wind speed < 8 m/s and near-bed orbital velocities < 0.6 m/s). For these conditions, wind-induced effects on the near-bed velocities can be neglected. The time series obtained from the flow meters were split up in four subseries with a length of 512 s each. Averaged values of these subseries were used for the comparisons with the model results.

Five different scenarios were defined using a combination of a bed form model, form roughness model and WC-model (see Table 1). A scenario with a fixed apparent bed roughness of 0.1 m was also used.

The flow model was run for these scenarios using the local grain size and the measured near-bed orbital velocity to compute the apparent bed roughness and the flow field. Here the average of the one-third highest peak orbital velocities obtained from the lower flow meter was used in the computation of the bed form dimensions and the wave–current interaction. An upper limit of the apparent roughness equal to the half of the water depth was applied to avoid infinite large roughness values for some scenarios during the turn of the tidal flow.

The flow velocities are computed for the whole period of 215 h at position P1 and P2 using all scenarios. The computed and predicted longshore velocities at 0.3 and 1.2 m above the bed are compared with each other and two statistical parameters were calculated to obtain insight in the quality of the flow predictions for each scenario. The first parameter is the slope of the least-square linear fit between the computed V_{computed} and measured velocity V_{measured}, defined by $V_{\text{computed}} = \gamma V_{\text{measured}}$. This parameter gives a good indication for the systematic error in the computed velocities. A γ-value close to one indicates a good average agreement between both variables and a value below (above) unity indicates a systematic under (over) prediction of the measured velocities and thus a roughness value which is too high (low). This parameter is calculated for each tripod-position and for the two flow levels separately (see Table 1). The standard deviation s around the best fit line is used as a measure for the spreading around the line.

The γ-values for scenario 5 with constant apparent roughness of 0.1 m vary within 5% of unity and the standard deviation of approximately 0.04 m/s is smaller than for the other scenarios. The application of scenario 1 yields slightly worse results. Scenario 2 results in over prediction of the measured velocities. Scenarios 3 and 4 result in considerable under prediction of measured velocities. Many other scenarios have been studied, yielding similar results. Analysis of the results show that the α-factor of the form roughness model $k_f = \alpha\eta(\eta/\lambda)$ has a relatively large effect on the computed velocities. Therefore, scenarios 3 and 4 were recalculated using $\alpha = 8$ (value proposed by Nielsen, 1981).This leads to a significant improvement of the results of these scenarios. Now the results of scenario 4 becomes the second best method. This indicates that the choice of the α-factor is a critical element in roughness prediction. The α-factors found in literature vary roughly between 10 and 30. Based on the results of the

Table 1
Definition of scenarios used in the flow computations

Scenario	Bed form model	Form roughness model	WC-model	γ-Parameter	Standard deviation s
1	Nielsen	Nielsen	G-M	0.9–1.1	0.045–0.055
2	Nielsen	Nielsen	Van Rijn	1.07–1.15	0.045–0.05
3	G-M	G-M	G-M	0.65–0.9	0.045–0.065
4	Van Rijn	Van Rijn	Van Rijn	0.75–0.95	0.05–0.06
5	$k_a = 0.1$ (constant)			0.95–1.05	0.035–0.045

present study, an α-factor of about 10 gives better results than α of about 30. Drake et al. (1992) also concluded that α of about 30 is too large based on measured bed form dimensions and the G-M WC-model. Others (e.g., Li and Amos, 1998) have found good results for an α-factor of about 30. Given these conflicting results, it is clear that some controlling parameters are missing. The missing parameters most likely are: bed form shape and angle between current direction and bed form orientation. Flume experiments on bed form shapes in unidirectional flow have shown that shape is a crucial parameter (Van Rijn, 1993). It can be expected that the presence of a current can result in a smoothing of wave-formed ripples, giving a substantial effect on the effective roughness. Furthermore, wave-dominated ripples will be oriented more or less perpendicular to the wave direction. A weak current under an angle of 90° with the waves will hardly experience any roughness from these ripples because the flow will pass the bed forms without generation of lee-side vortices. These two effects can be an explanation for the variation found by different researchers for the α-factor.

Fig. 5 shows an example of computed and measured velocities obtained from scenario 5 at position P2 for some part of the period considered. The most upper graph in Fig. 5 shows the measured near-bed orbital velocity which varies from 0.08 up to 0.58 m/s. The second graph of Fig. 5 shows the measured and computed longshore velocity at 1.2 m above the bed. Scenario 5 results in a rather accurate prediction of the measured velocities.

In this study, a fixed apparent bed roughness of 0.1 m yield the best results. To obtain some insight in the sensitivity of the computations using a fixed value of 0.1 m, the computations were repeated for fixed roughness values of 0.2 and 0.05 m, respectively. The computations based on a $k_a = 0.05$ m show a systematic overestimation of the flow

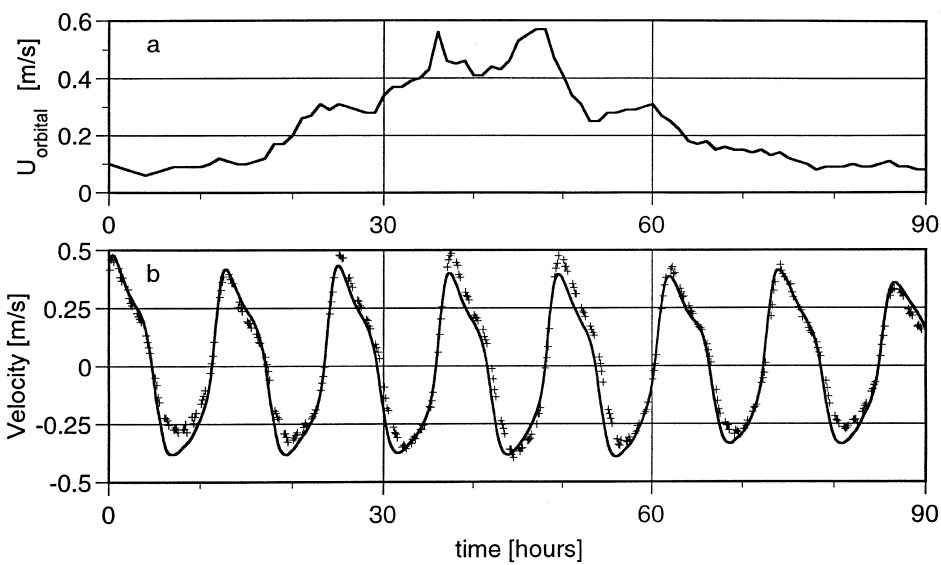

Fig. 5. Measured orbital velocities (a) and predicted and measured mean longshore velocity at 1.2 m above the bed (b).

velocity ($\gamma = 1.05–1.15$). The roughness value of 0.2 m results in predicted velocities lower ($\gamma = 0.85–0.95$) than the measured ones. The sensitivity of the computed near-bed velocities (an error of 10%–15% for a doubling or halving of the roughness value) seems to be moderate.

8. Conclusions

Modelling of the apparent bed roughness leads to realistic results, however, the final results are sensitive to the selection of the empirical models. The best choice for the apparent roughness turned out to be a fixed bed roughness of 0.1 m. The combination of the Nielsen (1981) bed form model and the Grant and Madsen (1979) WC-model gives roughness values which also lead to a rather accurate prediction of the measured velocities. In the ripple regime, the rather high form roughness is combined with a small amplification factor due to the wave–current interaction. In the sheet flow regime, a small physical roughness value is combined with a large amplification factor. The final result of this is a more or less constant apparent roughness value in both regimes. This is probably the reason why a constant apparent roughness value of 0.1 m gives good results for all calculations. The sensitivity of the computed velocities is moderate for apparent roughness values in the range of 0.05 to 0.2 m. The question remains how generally applicable the present finding of a fixed roughness value of 0.1 m is. On one hand, the analyses presented here are limited to typical mean flow conditions of 0.3 to 0.5 m/s, at 1.2 m above the bed and wave orbital velocities up to 0.6 m/s and wave periods ranging between 5 and 12 s. Observations at other sites show apparent roughness values which are 2 to 4 times higher than those found in this study. O'Connor et al. (1994) analysed data gathered at about 21 m water depth in front of the Belgian coastline. They found an apparent roughness k_a of 0.2–0.3 m for near-bed wave orbital velocities varying between 0.15 and 0.3 m/s. Drake et al. (1992) observed k_a ranging from 0.25 to 0.45 m during mean flow velocities of about 0.1 m/s at 1 m above the bed, with orbital velocities of approximately 0.1 m/s and wave period of 12 s. So, it is probably not true that a fixed apparent roughness of 0.1 m is always the optimal choice, especially for sites with significant different flow conditions and/or different bed material.

Future research on flow resistance should be focused on form roughness of ripples (α-factor) rather than on the prediction of ripple dimensions.

Acknowledgements

This work was carried in the framework of the NOURTEC project: Innovative Nourishment Techniques Evaluation. It was jointly funded by the Ministry of Transport, Public Works and Water Management in the Netherlands and by the Commission of the European Communities, Directorate General for Science, Research and Development under the Marine Science and Technology programme contract no. MAS2-CT93-0049.

References

Carstens, M.R., Neilson, R.M., Altinbilek, H.D., 1969. Bedforms generated in the laboratory under oscillatory flow: analytical and experimental study. U.S. Army Corps of Engineers, Coastal Engineering Research Center, Technical Memorandum 28, 39 pp.

Drake, D.E., Cacchione, D.A., Grant, W.D., 1992. Shear stress and bed roughness estimates for combined wave and current flows over a rippled bed. Journal of Geophysical Research 97 (C2), 2319–2326.

Grant, W.D., Madsen, O.S., 1979. Combined wave and current interaction with a rough bottom. Journal of Geophysical Research 84 (C4), 1797–1808.

Grant, W.D., Madsen, O.S., 1982. Movable bed roughness in unsteady oscillatory flow. Journal of Geophysical Research 87 (Cl), 469–481.

Grant, W.D., Madsen, O.S., 1986. The continental-shelf bottom boundary layer. Annual Review of Fluid Mechanics 18, 265–305.

Hoekstra, P., Houwman, K.T., Kroon, A., Van Vessem, P., Ruessink, B.G., 1994. The NOURTEC experiment of Terschelling: process-oriented monitoring of a shoreface nourishment (1993–1996). Proc. Coastal Dynamics 1994. ASCE, New York, pp. 402–416.

Houwman, K.T., Uittenbogaard, 1999. A comparison between modelled and measured tidal flow phenomena in the nearshore zone. Resubmitted to Journal of Physical Oceanography.

Li, M.Z., Amos, C.L., 1998. Predicting ripple geometry and bed roughness under combined waves and currents in a continental shelf environment. Continental Shelf Research 18, 941–970.

Li, M.Z., Wright, L.D., Amos, C.L., 1996. Predicting ripple roughness and sand resuspension under combined flows in a shoreface environment. Marine Geology 130, 139–161.

Nielsen, P., 1981. Dynamics and geometry of wave-generated ripples. Journal of Geophysical Research 86 (C7), 6467–6472.

Nielsen, P., 1992. Coastal bottom boundary layers and sediment transport. Advanced Series on Ocean Engineering, Vol. 4. World Scientific, Singapore.

O'Connor, B.A., Kim, H., Williams, J.J., 1994. Hydrodynamics of random wave boundary layers. Proc. Coastal Dynamics 1994. ASCE, New York, pp. 879–893.

Ribberink, J.S., Al-Salem, A.A., 1994. Sediment transport in oscillatory boundary layers in cases of rippled beds and sheet flow. Journal of Geophysical Research 99, 12707–12727.

Soulsby, R.L., Hamm, L., Klopman, G., Myrhaug, D., Simons, R.R., Thomas, G.P., 1993. Wave–current interaction within and outside the bottom boundary layer. Coastal Engineering 21, 41–69.

Van Rijn, L.C., 1993. Principles of sediment transport in rivers, estuaries and coastal seas. Aqua Publications, Amsterdam, the Netherlands.